Frontier molecular orbitals, MEP, NBO, and vibrational spectra of Mesalamine: A first principle study from DFT and molecular docking approaches

Manoj Kumar Chaudhary[*, **], Sudip Pandey[*] and Poonam Tandon[**]

[*]Department of Physics, Tribhuvan University, Amrit Campus, Institute of Science and Technology, Kathmandu, Nepal.

[**]Department of Physics, University of Lucknow, Lucknow-226007, India.

Abstract: The main purpose of this work is to investigate the structural, electronic, and vibrational features of mesalamine ($C_7H_7NO_3$) from density functional theory (DFT) approach. The optimized structure has been obtained from DFT calculation by using the functional B3LYP/ 6-311++G(d,p) basis set. The spectroscopic feature (FT-IR and FT-Raman) of the investigated compound has been calculated from the same level of theory. The molecular electrostatic potential (MEP) analysis is used to identify the distribution of charge around the compound. The highest occupied molecular orbital (HOMO) and lowest unoccupied molecular orbital (LUMO) have been studied and their energy gap (ΔE_{L-H}) is used to study the chemical potential (μ), hardness (η), softness(S) and electrofilicity index (ω) of the molecule. The electron transfer property has been scrutinized from natural bond orbital (NBO) analysis. Additionally, molecular docking was carried out to identify binding sites and the binding behavior of the ligand with a predicted target protein (Carbonic anhydrase II).

Keywords: Mesalamine; DFT; FT-IR; FT-Raman; HOMO-LUMO; MEP; Molecular docking.

Introduction

Mesalamine has molecular weight153.14 g/mol which is chemically known as 5-amino-2-hydroxybenzoic acid having molecular formula $C_7H_7NO_3$. It is widely used to treat inflammatory bowel disease in gastrointestinal tract infection by reducing colon edema[1]. In medication, mesalamine is classified from aminosalicylate which is known as mesalazine. It is commonly used to treat ulcerative colitis and Crohn's disease, two disorders of the inflammatory bowel[2]. The chemical structure of mesalamine is depicted in Figure 1.

Mesalamine alleviates the symptoms of inflammatory bowel diseases by reducing inflammation in the intestinal lining. It is thought to work specifically in the digestive tract's colon, which is where inflammation is most visible[3]. The detection of mesalamine drug from DFT by using the functional B3LYP was carried out to check the impact of Pd-decoration but the impact was found to be week moreover its detection from nanotubes method was identified from DFT approach[4,5]. The chemical sensors mainly works on the optoelectronic properties and it was carried on for polythiophen derivatives[6].

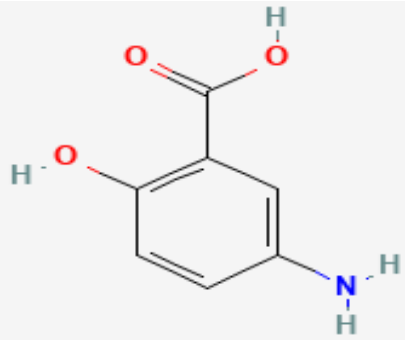

Figure 1: Chemical Structure of mesalamine.

The clinical activity of mesalamine has been studied by many research groups but structural activity such as geometry optimization, MEP, HOMO-LUMO, NBO, spectroscopy behavior, and molecular docking analysis is still the interest of study. Mainly these phenomena have been explored in this research.

Author for Correspondence: S.Pandey, Department of Physics, Tribhuvan University, Amrit Campus, Institute of Science and Technology, Kathmandu, Nepal.
Email: pandeysudipg@gmail.com; https://orcid.org/0009-0006-3432-7564
Received: 19 May, 2024; Received in revised form: 03 Jun, 2024; Accepted: 04 Jun, 2024.
Doi: https://Doi.org/10.3126/sw.v17i17.66417

Computational details

The title compound has been computationally evaluated using the Gaussian 09 software and optimization was done using the Gaussian 09 default settings[7]. The optimized structure of the evaluated compound was performed using the functional B3LYP and 6-311++G(d,p) basis sets by implementing the DFT theory of calculation[8-11]. Moreover, the NBO, MEP, HOMO-LUMO, and Mulliken charges have been estimated at the same theoretical level as optimization. The charge distribution inside the molecule was seen using the GaussView05 program[12]. Molecular docking simulations were carried out by Auto Dock Tools (ADT) version 4.2, including binding energy, ligand efficiency, and inhibition constant[13]. The mesalamine molecule was docked with the protein targets and visualization was done with the Discovery Studio program's LIGPLOT tool[14].

Results and discussion

Geometry optimization

The 3-D optimized structure of mesalamine with atom numbering is presented in Figure 2. The ground state energy was obtained as -551.5613 a.u. The bond lengths and bond angles at B3LYP/6-311++G(d,p) of mesalamine were compared with the experimental values of mono-substituted salicylic acid whose structure is similar to that of mesalamine is presented in Table 1. Their calculated values are in good agreement with the experimental one[15]. The optimized structure's dipole moment was obtained as 4.067 Debye. The pull between the two atoms is stronger and the bond length is shorter for higher bond orders. The bond lengths of N4-C6, N4-H15, and N4-H16 are 1.403 Å, 1.009 Å, and 1.010 Å. Every molecule's bond length agrees well with the optimal structure. Similarly, the greatest bond length of the optimized structure, 1.485 Å, is seen for the C-C bond length, which falls within this range.

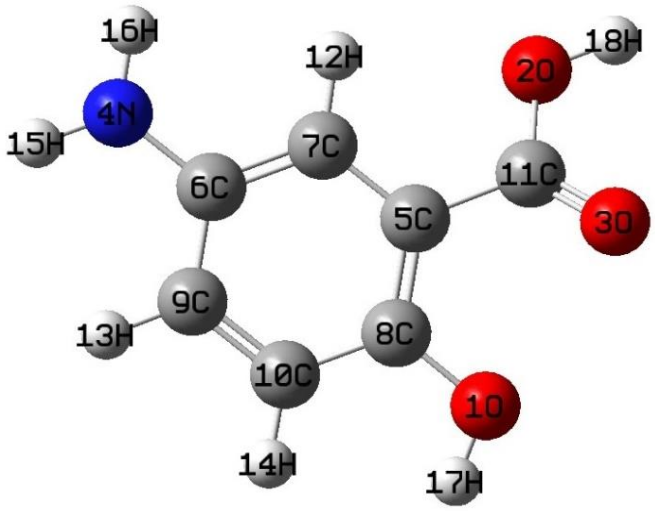

Figure 2: 3-D Structure of mesalamine with atom numbering.

Table1: Bond length, and bond angle of mesalamine and experimental value of bond length and bond angle of literature[15].

	Bond length (Å)			Angle (˚)	
Bonds	Theoretical	Experimental Literature[15]	Bonds	Theoretical	Experimental Literature[15]
O1-C8	1.361	1.363	C8-O1-H17	108.98	109.07
O1-H17	0.963	0.973	C11-O2-H18	105.77	111.86
O2-C11	1.3692	1.360	C6-N4-H15	115.03	120.02
O2-H18	0.9678	0.981	C6-N4-H16	114.86	120.06
O3-C11	1.206	1.234	H15-N4-H16	111.29	119.91
N4-C6	1.404	1.410	C7-C5-C8	118.97	119.99
N4-H15	1.010	1.011	C7-C5-C11	119.62	11.16
N4-H16	1.010	1.011	C8-C5-C11	121.40	120.84
C5-C7	1.405	1.395	N4-C6-C7	121.17	119.98
C5-C8	1.409	1.395	N4-C6-C9	120.88	120.01
C5-C11	1.485	1.456	C7-C6-C9	117.86	120.01
C6-C7	1.3933	1.395	C5-C7-C6	122.31	120.00

C6-C9	1.402	1.395	C5-C7-H12	118.06	121.03
C7-H12	1.082	1.088	C6-C7-H12	119.63	118.97
C8-C10	1.398	1.395	O1-C8-C5	120.26	120.88
C9-C10	1.387	1.395	O1-C8-C10	121.07	119.12
C9-H13	1.085	1.087	C5-C8-C10	118.66	120.88
C10-H14	1.086	1.087	C6-C9-C10	120.66	120.00
			C6-C9-H13	119.92	120.70
			C10-C9-H13	119.41	119.31
			C8-C10-C9	121.52	120.01
			C8-C10-H12	119.07	
			C9-C10-H14	119.40	119.21
			O2-C11-O3	120.89	122.26
			O2-C11-C5	112.11	112.40
			O3-C11-C5	126.99	125.34

Natural bond orbital (NBO) analysis

Natural bond orbital (NBO) analysis has been used to check the delocalization of charge from the donor to the acceptor level. The stabilization energy E(2) which determines delocalization electron from donor to acceptor is the major parameter to check the donor (i) to acceptor (j) orbitals. Table 2 presents the calculated value of E(2) for mesalamine between prominent bonding and antibonding orbitals, as determined by the diagonal element of the Fock matrix from second-order perturbation theory and is given by[16-19].

$$E^{(2)} = E\,(i, j) = -q_i \frac{(Fi,j)^2}{Ej - Ei} \quad (1)$$

where $F_{i,j}$ is the off-diagonal element of the Fock matrix, q_i is the occupancy of natural bond orbitals, E_i is the energy of the donor orbital and E_j is the energy of the acceptor orbital. Second-order perturbation analysis of the Fock matrix yields the various donor-acceptor interaction types and their equilibrium energies, which are listed in Table 2. The molecule experiences resonance as a result of the interaction π(C5-C8) → π∗(O3-C11), yielding a stability energy of 23.08 kcal/mol. The lone pair LP(2)O2 → π∗(O3-C11) has been shown to interact very strongly, stabilizing the molecule with a stabilization energy of 44.66 kcal/mol. With energies of 26.43 kcal/mol, the lone pair LP (1) N4 takes part in the charge transfer from LP(1)N4 → π∗(C6-C7). The stabilization energy resulting from the interactions LP(2)O1 → π∗(C5-C8) is 31.64 kcal/mol.

Table 2: Second-order perturbation theory analysis of the Fock matrix in NBO basis of the mesalamine.

Donor NBO(i)	ED(i)/e	Acceptor NBO(j)	ED(j)/e	[a]E(2) kcal/mol	[b][E(j)-E(i)] a.u.	[c]F(i,j) a.u.
σ(O1-H17)	-0.74755	σ∗(C5-C8)	0.55536	5.36	1.30	0.075
π(C5-C8)	-0.25807	π∗(O3-C11)	-0.00216	22.56	0.26	0.070
π(C5-C8)	-0.25807	π∗(C6-C7)	0.02859	20.98	0.29	0.069
π(C5-C8)	-0.25807	π∗(C9-C10)	0.01994	19.35	0.28	0.066
π(C6-C7)	-0.25385	π∗(C5-C8)	0.01658	19.39	0.27	0.066
π(C6-C7)	-0.25385	π∗(C9-C10)	0.01994	21.75	0.27	0.069
π(C9-C10)	-0.26107	π∗(C5-C8)	0.01658	20.51	0.28	0.071
π(C9-C10)	-0.26107	π∗(C6-C7)	0.02859	17.25	0.29	0.065
LP(1)O1	-0.56678	σ∗(C8-C10)	0.55926	5.77	1.13	0.072

LP(2)O1	-0.31171	π∗(C5-C8)	0.01658	31.24	0.33	0.098
LP(1)O2	-0.59162	σ∗(O3-C11)	0.58537	6.19	1.18	0.076
LP(2)O2	-0.32432	π∗(O3-C11)	-0.00216	44.66	0.32	0.110
LP(2)O3	-0.25389	σ∗(O2-C11)	0.29567	37.6	0.55	0.130
LP(2)O3	-0.25389	σ∗(C5-C11)	0.43608	19.19	0.69	0.105
LP(1)N4	-0.27909	π∗(C6-C7)	0.02859	26.43	0.31	0.086
π∗(O3-C11)	-0.00216	π∗(C5-C8)	0.01658	135.39	0.02	0.075
π∗(C5-C8)	0.01658	π∗(C6-C7)	0.02859	273.39	0.01	0.079

[a]E(2) = Stabilization energy.

[b][E(j)-E(i)] = Energy difference between donor (i) and acceptor (j) NBO orbitals.

[c]F(i,j) = Fock matrix element between i and j NBO orbitals.

Vibrational spectra

The mesalamine molecule with 18 atoms can vibrate in 48 (3N–6) normal modes. They are all both infrared and Raman active modes. Since Raman amplitudes are not produced by the quantum chemical computation, Raman intensities were calculated for each normal mode of vibration using the Raman scattering cross-section, $\partial\sigma_j/\partial\Omega$, and are provided by the relation[20] ,

$$\frac{\partial\sigma j}{\partial\Omega} = \left(\frac{2^4\pi^4}{45}\right)\left(\frac{(\nu o-\nu j)^4}{1-\exp\left[\frac{-hcvj}{kT}\right]}\right)\left(\frac{h}{8\pi^2 cvj}\right)Sj \qquad (2)$$

where, Sj = scattering activities, νj = predicted wavenumbers for j th normal mode, νo = wave number of Raman excited state, and h, c, and k are universal constants. A Lorentzian line shape (FWHM = 8 cm^{-1}) is used to produce simulated spectra from the calculated Raman and IR intensities by convoluting the predicted vibrational mode. The FT-IR and FT-Raman graph of mesalamine is presented in Figures 3 and 4

O-H vibrations

The (O-H) group's stretching vibration falls between (3100 - 3690) cm^{-1} [21]. We have detected the hydroxyl stretching at 3502 and 3510 cm^{-1} in our study. Similarly, bending was noted at 658 cm^{-1}.

N-H vibrations

In both the IR and Raman spectra, the amine group (NH_2)'s N-H asymmetric stretching mode was detected at 3435 cm^{-1}. The estimated value of 3434 cm^{-1} was in good agreement with the experimental value[22]. Although it was not seen in the experimental spectra, the N-H stretching in the computed spectra was estimated at 3424 cm^{-1}. The estimated N-H inplane bending vibration (scissoring) of N4H16 at 1597 cm^{-1} in both IR and Raman spectra suggests a good agreement between the theoretical and experimental spectra. This group's rocking vibration was measured at 1116 $cm^{-1}$and seen at 1113 cm^{-1}in the Raman and IR spectra, respectively.

C-H vibrations

The CH_2 group has a wiggling vibration range of (1368-1300) cm^{-1}[22]. The frequency of wagging is calculated to be 1362 cm^{-1}. We observe the symmetric stretching frequency of CH_2 at 3198 cm^{-1} and the asymmetric stretching frequency at 3175 cm^{-1}. In the Raman band, both are present. Nonetheless, in the infrared band, the twisting and rocking are indicated at 806 cm^{-1} and 944 cm^{-1}, respectively.

Benzene ring vibration

The C-H stretching vibrations of aromatic compounds are generally measured in the range of (3100 to 3200) cm^{-1} [23]. C-H stretching was used to calculate the IR spectra at 3175 and 3248 cm^{-1} and 3093 and 3061 cm^{-1}, respectively. In the IR and Raman spectra, the ν(CC) ring stretching was clearly identified at 1305 cm^{-1}, after being measured at 1327 cm^{-1}.

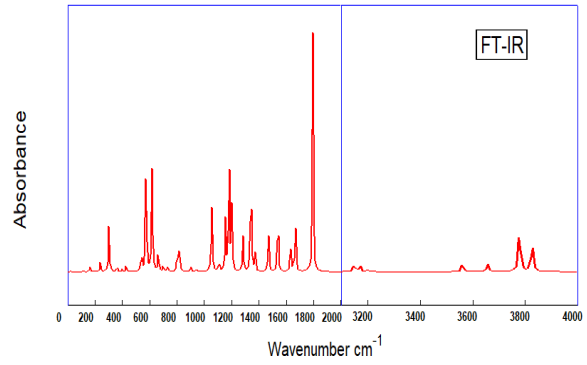

Figure 3: The calculated FT- IR spectrum of mesalamine.

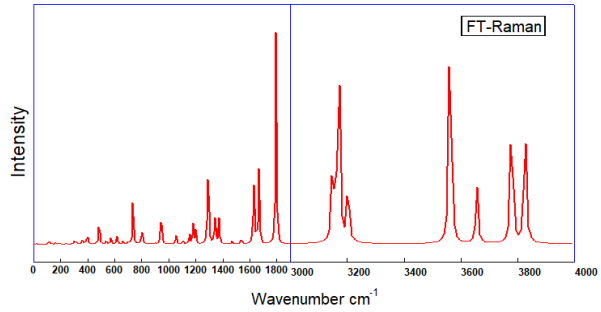

Figure 4: The calculated FT- Raman spectrum of mesalamine.

Molecular electrostatic potential (MEP) surface

MEP analysis can be used to anticipate the active medicinal ingredient's reactive sites. The development of a dipole moment across a molecule and the dispersion of electron density in space around it are best understood visually using the MEP approach. The equation indicates the molecular electrostatic potential V(r) generated throughout the molecule as a result of the combined action of positive and negative charges corresponding to electrons and nuclei[24].

$$V(r) = \sum_A \frac{ZA}{|\vec{RA} - \vec{r}|} - \int \frac{\rho(\vec{r'})}{|\vec{r'} - \vec{r}|} \quad (3)$$

where ZA is the charge on nucleus A, present at R_A, and ρ(r′) is the electronic density function of the molecule. The electrostatic potential is determined by the color code, where red indicates the highest negative potential, blue indicates the highest positive potential, and green indicates the zero-potential region. Red < yellow < green < blue is the increasing order of the potential distribution in the MEP map. Figure 5 shows the mesalamine MEP map color-coded. The strongest positive potential and the most intense blue patches are exhibited by hydrogen atoms H15 and H16 across the amine group (NH_2), which are also in charge of nucleophilic assault on neighboring species. The electrophilic attack of mesalamine is caused by the oxygen atom across the carbonyl group (C11=O), which has a red area with the largest negative potential.

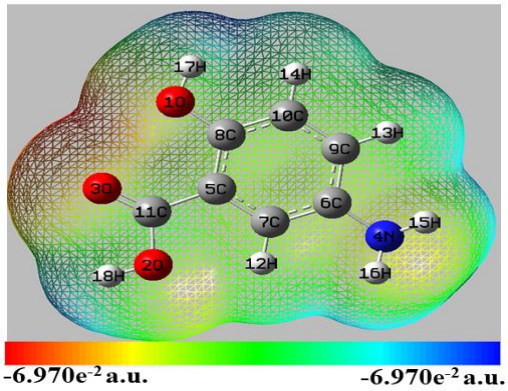

Figure 5: Molecular electrostatic potential (MEP) surface map of mesalamine.

UV-Vis and frontier molecular orbital analysis

The chemical and optical properties of organic compound can be described from UV-Vis and frontier molecular orbital analysis. In molecular system the highest occupied molecular orbital (HOMO) and the lowest unoccupied molecular orbital (LUMO) have prominent role in chemical reaction[25]. The stability and chemical reactivity of the molecule are measured by the energy of the LUMO orbital (E_L) and the HOMO orbital (E_H), as well as their energy gap (ΔE_{L-H}). A higher value of ΔE_{L-H} suggests that the molecule is less reactive and more stable, and vice versa [26]. The time dependent DFT (TD-DFT) have been implemented to calculate HOMO, HOMO–1, HOMO–2, LUMO, LUMO+1and LUMO+2 at B3LYP/6-311++G(d,p) level of theory. The HOMO, HOMO–1, HOMO–2, LUMO, LUMO+1and LUMO+2 plot gas phase is presented in Figure 6.

The value of ΔE_{L-H} for the mesalamine compound is 2.9158 eV when calculated at the B3LYP/6–311++G(d,p) level of theory. It is evident that the HOMO charge is confined across rings, while the LUMO orbital lobes likewise diverge to the amine group and rings in LUMO.

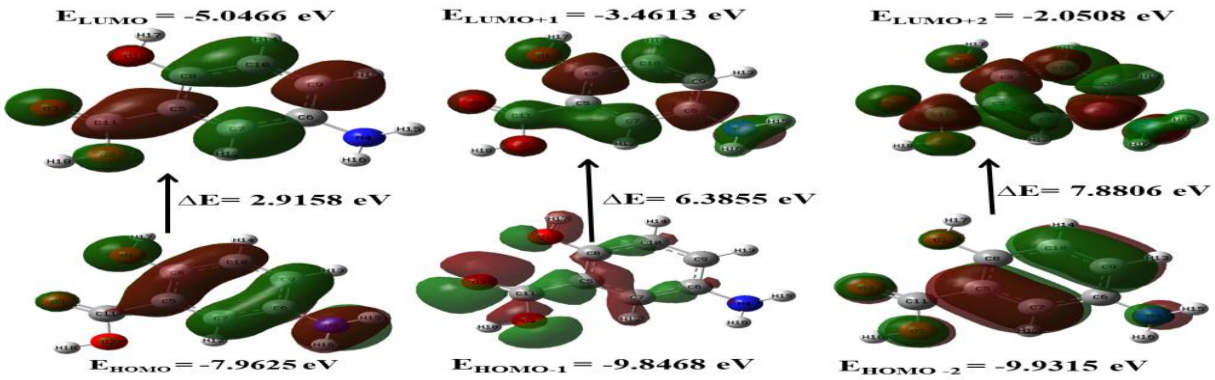

Figure 6: HOMO-LUMO plots of mesalamine.

Theoretically, the UV-Vis spectra of mesalamine is calculated at TD-DFT from B3LYP/6-311++G(d,p) level of theory. Four absorption peaks are calculated in the UV-Vis spectra. The first peak is obtained at 147 nm wavelength which is due to transition from HOMO-1 to LUMO+3 with excitation energy 8.4258 eV. Another peak is calculated at 171 nm wavelength with excitation energy 7.2148 eV, this is due to transition from HOMO-2 to LUMO+1. The prominent peak is calculated at 198 nm wavelength and another peak is calculated at 326 nm wavelength. The UV-Vis spectrum of mesalamine is presented in Figure 7.

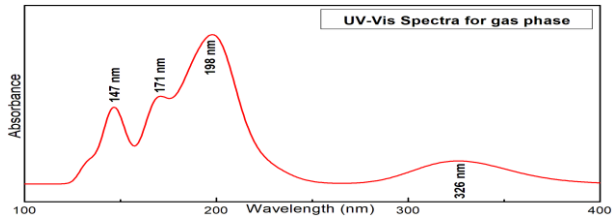

Figure 7: UV-Vis spectra of mesalamine in gas phase.

Global reactivity descriptor

Koopman's theorem suggests the following global reactivity parameters: electronegativity (χ), chemical potential (μ), hardness (η), electrophilicity index (ω), and softness (S). These values are determined using the molecular orbital energies (E_H and E_L) of the frontier, which are provided by the following relations[27,28]:

$$\chi = -\frac{1}{2}(E_{HOMO} + E_{LUMO}) \quad (4)$$

$$\mu = -\chi = \frac{1}{2}(E_{HOMO} + E_{LUMO}) \quad (5)$$

$$\eta = -\frac{1}{2}(E_{HOMO} - E_{LUMO}) \quad (6)$$

$$S = \frac{1}{2\eta} \quad (7)$$

$$\omega = \frac{\mu 2}{2\eta} \quad (8)$$

According to Parr et al., ω is expressed in terms of μ and η, which are always positive and indicate the energy stabilization that occurs when the system picks up an additional charge (ΔN) from a nearby molecule. The good electrophilic/nucleophilic behavior of molecules is indicated by a high/low value of μ and ω, respectively. Table 3 lists the mesalamine's computed values for E_H, E_L, ΔE_{L-H}, χ, μ, η, ω, and S.

Table 3: Calculated E_{HOMO}, E_{LUMO}, energy gap (ΔE_{L-H}), chemical potential (μ), electronegativity (χ), global hardness (η), softness (S) and electrophilicity index (ω) of mesalamine.

E_H (eV)	E_L(eV)	ΔE_{L-H} (eV)	χ (eV)	μ (eV)	η (eV)	$S(eV)^{-1}$	ω(eV)
-7.9625	-5.0466	2.9158	6.5045	-6.5045	1.4579	0.3429	14.5100

Mulliken Charge

Partial atomic charges are provided by the Mulliken charges[29]. They are specifically affected by the basis set selection made for the theoretical computation. They provide the associated atoms with qualitative results of the charge distribution. More dependable, the Mulliken charges control the electron density. Atomic orbitals that are

localized can be utilized to explain electron density. In contrast to the Mulliken system, which does not take polarization into account, this technique takes into account the polarization bonds. The Mulliken charges acquired using the basis set B3LYP/6-311++G(d,p). Figure 8 displays a graphical representation of them. C5 atom has most positive concentration of charge whereas the C8 atom has most negative concentration of charge.

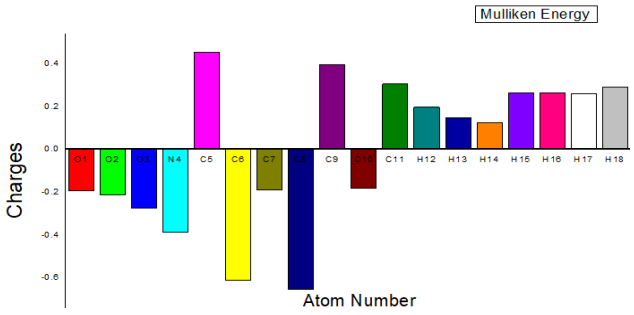

Figure 7: The calculated Mulliken charge of mesalamine.

Molecular docking

Molecular docking is a technique used to display how drug molecules attach to proteins[30]. Mesalamine acts as a pharmaceutical treatment for inflammatory bowel disease. Despite being beneficial in treating and preserving remission for ulcerative colitis, it has not yet been studied how to dock this compound with the CA2 (Carbonic anhydrase II) receptor for therapeutic purposes. The online Swiss target prediction predicts the receptor CA2[31,32]. The PDB code 4XIX has been downloaded from protein data bank[33]. The protein was purified by eliminating the water molecules, and its active site was confined into a 60 Å x 60 Å x 60 Å grid box. The binding energy, bond lengths of typical H-bonds with residues, and binding efficiencies for docked conformation is presented in Table 4. Figure 9 shows a visual representation of the ligand's binding sites with the protein. The binding sites are typically discovered to be the carboxyl group OH and amine NH_2. With four typical H-bonds (1.219 Å / ASN:104, 1.241 Å /THR:293, 1.233 Å / VAL:285, 1.236 Å /ASP:287), the PDB code 4XIX exhibits a stable binding energy of -5.83 kcal/mol. Therefore, it is theoretically possible to expect that mesalamine has strong antimigraine properties. To validate its actions, additional in vitro and in vivo research must be done.

Table 4: Hydrogen bonding, binding energy and ligand efficiency of mesalamine with predicted targets.

ligand	Protein	PDB Code	Bond Length	Amino Acid	Binding Energy (kcal/mol)	Ligand efficiency
Mesalamine	Carbonic Anhydrase II	4XIX	1.219 1.241 1.233 1.236	ASN:104 THR:293 VAL:285 ASP:287	-5.83	-0.31

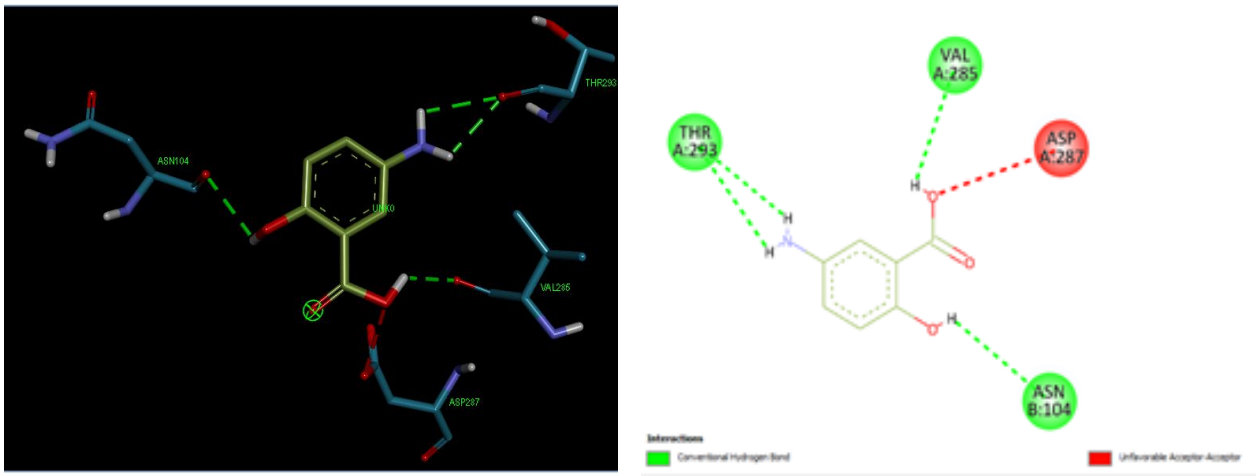

Figure 8. Molecular Docking of mesalamine with protein targets Carbonic Anhydrase I.

Conclusion

Quantum chemical calculation and vibrational spectroscopic properties were done on mesalamine. The minimum energy of the investigated compound at DFT/B3LYP/6–311++G(d,p) level of theory was found to be -551.5613 a.u and its bond lengths and bond angle are in good agreement with experimental data of mono-substituted salicylic acid. A comparison between the estimated IR and Raman data with experimental data of functional group in literature reveals a strong resonance between them. The NBO analysis shows that the chemical system with the highest stabilization energy 273.09 kcal/mol is stabilized by the transition $\pi*(C5\text{-}C8) \rightarrow \pi*(C6\text{-}C7)$. The frontier molecular orbital research revealed that the energy HOMO and LUMO, respectively, was -7.9625 eV and -5.0466 eV. The value of the HOMO-LUMO energy gap $\Delta E_{L\text{-}H}$ is determined to be 2.9158 eV. Concurrently, the values of 6.5045, -6.5045, 1.4579, and 14.5100 eV have been obtained for the global reactivity parameters, which include electronegativity (χ), chemical potential (μ), global hardness (η), and global electrophilicity index (ω) respectively. We find that the global softness (S) is 0.3429 eV^{-1}. The electrostatic potential surface map makes it evident that the electrophilic center is represented by the red patches, which are localized over nitrogen and oxygen, while the largest positive potential (blue) is located over the nitrate group, which functions as a nucleophilic center. As a result, we can identify the reactive sites for molecular docking by knowing the nucleophilic and electrophilic sites on the molecular electrostatic potential surface. The mesalamine molecule binds to the chosen targets with a higher binding energy and is projected to have a lower inhibition constant, according to docking analysis. The amine (NH_2) group is discovered to be mesalamine's binding site, and this finding is correlated by the C5 atom having the highest positive charge whereas the C8 atom has the highest negative charge in Mulliken charges analysis.

Acknowledgments

M.K. Chaudhary is grateful to DST, India for providing partial financial support under the Indian Science and Research Fellowship (INSA/DST-ISRF/2023/NEP/08/13).

References

1. Bayan, M. F. and Bayan, R. F. 2020. Recent advances in mesalamine colonic delivery systems. *Future Journal of Pharmaceutical Sciences*. **6**(1): 43.
   Doi: doi.org/10.1186/s43094-020-00057-7
2. Nduma, B. N., Mofor, K. A., Tatang, J., Ekhator, C., Ambe, S. and Fonkem, E. 2023. The use of cannabinoids in the treatment of inflammatory bowel disease (IBD): a review of the literature. *Cureus*. *15*(3): e36148. PMID: 37065370; PMCID: PMC10101654.
   Doi: 10.7759/cureus.36148
3. Santos, Y. and Jaramillo, A. P. (2023). Effectiveness of mesalamine in patients with ulcerative colitis: a systematic review. *Cureus*. *15*(8).
   Doi: 10.7759/cureus.44055
4. Yang, H., Jiang, Z., Liu, L., Zeng, Y. and Ebadi, A. G. 2022. A DFT study on the Pd-decorated AlP quantum dots as chemical sensor for recognition of mesalamine drug. *Phosphorus, Sulfur, and Silicon and the Related Elements*. **197**(7): 732-740.
   Doi: doi.org/10.1080/08927022.2021.2025234
5. Olegovich Bokov, D., Jalil, A. T., Alsultany, F. H., Mahmoud, M. Z., Suksatan, W., Chupradit, S. and Delir Kheirollahi Nezhad, P. 2022. RETRACTED ARTICLE: Ir-decorated gallium nitride nanotubes as a chemical sensor for recognition of mesalamine drug: a DFT study. *Molecular Simulation*. **48**(5): 438-447.
   Doi: doi.org/10.1080/08927022.2021.2025234
6. Barboza, B. H., Gomes, O. P. and Batagin-Neto, A. (2021). Polythiophene derivatives as chemical sensors: a DFT study on the influence of side groups. *Journal of Molecular Modeling*, *27*(1): 17.
   Doi: https://doi.org/10.1007/s00894-020-04632-w
7. M.J. Frisch, G.W. Trucks, H.B. Schlegel. G.E. Scuseria, J.R. Cheeseman, M.A. Robb, G. Scalmani, V. Barone, B. Mennucci, G.A. Petersson, H. Nakatsuji, M. Caricato, X. Li, H.P. Hratchian, A.F. Izmzylov, J. Bloino, G. Zheng, J.L. Sonnenberg, M. Hada, M. Ehara, K. Toyota, R. Fukuda, J. Ishida, M. Hasegawa, T. Nakajima, Y. Honda, O. Kitao, H. Nakai, T. Vreven, J.A. Montgomery Jr., J.E. Peralta, F. Ogliaro, M. Bearpark, J.J. Heyd, E. Brothers, K.N. Kudin, V.N. Staroverov, R. Kobayashi, J. Normand, A. Raghavachari, A. Rendell, J.C. Burant, S.S. Iyengar, J. Tomasi, M. Cossi, N. Rega, J.M. Millan, M. Klene, J.E. Knox, J.B. Cross, V. Bakken, C. Adamo, J. Jaramillo, R. Gomperts, R.E. Stratmann, O. Yazyev, A.J. Austin, R. Cammi, C. Pomelli, J.W. Ochterski, R.L. Martin, K. Morokuma, V.G. Zakrzewski, G.A. Voth, P. Salvador, J.J. Dannerberg, S. Dapprich, A.D. Daniels, J. Farkas, B. Foresman, J.V. Ortiz, J. Cioslowski, D.J. Fox, GAUSSIAN 09, Revision, Gaussian, Inc., Wallingford CT, (2009).

8. Hohenberg ,P., Kohn,W. 1964. Inhomogeneous Electron Gas. *Phys. Rev.* **B 136**: 864–871. Doi: https://doi.org/10.1103/PhysRev.136.B864
9. Lee, C.T., Yang, W.T., Parr, R.G.1988. Development of the Colle-Salvetti correlation-energy formula into a functional of the electron density. *Phys. Rev. B Condens. Matter*. **37:** 785–789. Doi: https://doi.org/10.1103/PhysRevB.37.785
10. Becke, A.D. 1993. Density-functional thermochemistry. III. The role of exact exchange. *J. Chem. Phys.* **98**: 5648–5652. Doi: 10.1063/1.464913
11. T.H. Dunning Jr. 1989. Gaussian basis sets for use in correlated molecular calculations. I. The atoms boron through neon and hydrogen. *J. Chem. Phys.* **90**: 1007–1023. Doi: https://doi.org/10.1063/1.456153
12. Frisch, A., Nielson, A.B., Holder, A.J. 2005. GaussView User Manual, Gaussian Inc, Pittsburgh, PA.
13. Trott, O., Olson, A.J. 2010. AutoDock Vina: improving the speed and accuracy of docking with a new scoring function, efficient optimization, and multithreading. *J. Comput. Chem*. **31**: 455–461. Doi: https://doi.org/10.1002/jcc.21334
14. Discovery Studio 4.5 Guide, Accelrys Inc. 2009. San Diego. http://www.accelrys.com.
15. Montis, R. and Hursthouse, M. B. 2012. Surprisingly complex supramolecular behaviour in the crystal structures of a family of mono-substituted salicylic acids. *CrystEngComm*. **14**(16): 5242-5254. Doi: doi.org/10.1039/C2CE25336D
16. Reed, A.E., Weinhold, F. 1983. Natural bond orbital analysis of near-Hartree–Fock water dimer, J. Chem. Phys. **78**: 4066−4073. Doi: https://doi.org/10.1063/1.445134
17. Weinhold, F., Landis, C.R. 2005. Valency and Bonding: A Natural Bond Orbital Donor– Acceptor Perspective, Cambridge University Press, Cambridge.
18. Reed, A.E., Curtis, L.A.. 1988. Weinhold, Intermolecular interactions from a natural bond orbital, donor-acceptor viewpoint. *Chem. Rev.* 88: 899–926. Doi: https://doi.org/10.1021/cr00088a005
19. Joshi, B. D., Thakur, G. and Chaudhary, M. K. 2021. Molecular structure, homo-lumo and vibrational analysis of ergoline by density functional theory. *Scientific World*. **14**(14): 21-30. Doi: https://doi.org/10.3126/sw.v14i14.34978
20. Guirgis, G.A., Klaboe, P., Shen, S., Powell, D.L., Gruodis, A., Aleksa, V., Nielsen, C.J., Tao, J., Zheng, C., Durig, J.R. 2003. Spectra and structure of silicon-containing compounds. XXXVI—Raman and infrared spectra, conformational stability, ab initio calculations and vibrational assignment of ethyldibromosilane. *J. Raman Spectrosc*. **34(4)**: 322–336. Doi: https://doi.org/10.1002/jrs.989
21. Colthup, N.B., Daly, L.H., Wiberley, S.E. 1990. Introduction to Infrared and Raman Spectroscopy, Academic Press, New York.
22. Varsányi, G. (1973). *Assignments for vibrational spectra of 700 benzene derivates*. Akademiai Kiado.
23. Thamarai, A., Vadamalar, R., Narayana, M. S., Ramesh, B. P., Muhamed, R.R., Sevvanthi, S., Aayisha, S. 2020. Molecular structure interpretation, spectroscopic (FT-IR, FT-Raman), electronic solvation (UV–Vis, HOMO-LUMO and NLO) properties and biological evaluation of (2E)-3-(biphenyl-4-yl)-1-(4-bromophenyl) prop-2-en-1-one: Experimental and computational modeling approach. *Spectrochim. Acta A Mol. Biomol. Spectrosc*. **226**: 117609. Doi: https://doi.org/10.1016/j.saa.2019.117609
24. Weiner, P.K., Langridge, R., Blaney, J.M., Schaefer, R., Kollman, P.A. 1982. Electrostatic potential molecular surfaces. *Proc. Natl. Acad. Sci:*. U.S.A.**79**: 3754−3758. Doi: https://doi.org/10.1073/pnas.79.12.3754
25. Chaudhary, M. K., Chaudhary, T. and Joshi, B. D. 2021. Simulated spectra (IR and Ra- man), NLO, AIM and molecular docking of carisoprodol from DFT approach. *BIBECHANA*. **18**: 48–57. Doi: doi.org/10.3126/bibechana.v18i1.29036
26. Chaudhary, M. K., Karthick, T., Joshi, B. D., Prajapati, P., de Santana, M. S. A., Ayala, A. P., and Tandon, P. 2021. Molecular structure and quantum descriptors of cefradine by using vibrational spectroscopy (IR and Raman), NBO, AIM, chemical reactivity and molecular docking. *Spectrochimica Acta Part A: Molecular and Biomolecular Spectroscopy*. 246: 118976. Doi: https://doi.org/10.1016/j.saa.2020.118976
27. Chaudhary, T., Chaudhary, M. K., Jain, S., Tandon, P., and Joshi, B. D. 2023. The experimental and theoretical spectroscopic elucidation of molecular structure, electronic properties, thermal analysis, biological evaluation, and molecular docking studies of isococculidine. *Journal of Molecular Liquids*. **391**: 123212. Doi: doi.org/10.1016/j.molliq.2023.123212
28. Parr, R.G., Yang, W. 1989. Density Functional Theory of Atoms and Molecules, Oxford University Press, New York.
29. Shalya, D., and Kumar, S. 2023. Molecular geometry, homo-lumo analysis and mulliken charge distribution of 2, 6-dichloro-4-fluoro phenol using DFT and HF method. *East European Journal of Physics*. 1: 205-209. Doi: doi.org/10.26565/2312-4334-2023-1-27
30. Chaudhary, M. K., Srivastava, A., Singh, K. K., Tandon, P., & Joshi, B. D. 2020. Computational evaluation on molecular stability, reactivity, and drug potential of frovatriptan from DFT and molecular docking approach. *Computational and Theoretical Chemistry*. **1191**: 113031. Doi: https://doi.org/10.1016/j.comptc.2020.113031
31. Chaudhary, M. K., Prajapati, P., Srivastava, K., Silva, K. F., Joshi, B. D., Tandon, P., & Ayala, A. P. 2021. Molecular

interactions and vibrational properties of ricobendazole: Insights from quantum chemical calculation and spectroscopic methods. *Journal of Molecular Structure.* **1230**: 129889. Doi: https://doi.org/10.1016/j.molstruc.2021.129889

32. Daina, A., Michielin, O., Zoete, V. 2019. SwissTargetPrediction: updated data and new features for efficient prediction of protein targets of small molecules. *Nucleic Acids Res.* **47(W1)**: W357−W364. Doi: https://doi.org/10.1093/nar/gkz382
33. Rose, P.W., Beran, B., Bi, C., Bluhm, W.F., Dimitropoulos, D., Goodsell, D.S., Prlić, A., Quesada, M., Quinn, G.B., Westbrook, J.D., Young, J. 2010. The RCSB Protein Data Bank:redesigned web site and web services, Nucleic Acids Res. **39** D392–D401. Doi: https://doi.org/10.1093/nar/gkq1021